This is a version of an article accepted for publication/published in IJSCD.
The Version of Record is available online at International Journal of Spray and Combustion Dynamics 2(2):125–149, 2010, http://doi.org/10.1260/1756-8277.2.2.125

Laser-based Spatio-temporal Characterisation of Port Fuel Injection (PFI) Sprays

Anand T. N. C., Devendra Deshmukh, Madan Mohan A. and Ravikrishna R. V.
Department of Mechanical Engg., Indian Institute of Science, Bangalore 560012, India
Email: ravikris@mecheng.iisc.ernet.in

[Received date; Accepted date]

Abstract
In the present work, detailed laser-based diagnostic experiments were conducted to characterise the spray from low pressure 2-hole and 4-hole Port Fuel Injection (PFI) injectors. The main objective of the work included obtaining quantitative information of the spatio-temporal spray structure of such low-pressure gasoline sprays. A novel approach involving a combination of techniques such as Mie scattering, Granulometry, and Laser Sheet Dropsizing (LSD) was used to study the spray structure. The droplet sizes, distributions with time, Sauter Mean Diameters (SMD), droplet velocities, cone angles and spray tip penetrations of the sprays from the injectors were determined. The spray from these injectors is found to be 'pencil like' and not dispersed as in high pressure sprays. The application of the above mentioned techniques provide two-dimensional SMD contours of the entire spray at different instants of time, with reasonable accuracy.

1. INTRODUCTION

Stringent emission norms have been driving developments in technology in internal combustion engines. While emission norms for small four-stroke engines in India are among the most stringent in the world, experimental and modelling studies on manifold processes, which dictate the performance and emission formation to a large extent, have not received much attention in literature. Over the last few years, low-pressure (~2.5 bar) PFI injection systems are being looked at as an alternative to the carburetor for small, four-stroke IC engines in two-wheeler applications. While the injection process in PFI engines has been studied experimentally by various groups, the studies have mostly focused on large engines. Fewer studies are found on small two-wheeler engines. Earlier studies on PFI sprays include those by Lenz [1], who discusses the different types of injectors and their operation characteristics: Pintle-type injectors give a cone-shaped spray while single-hole-type injectors form pencil-shaped sprays. Multi-hole-type injectors may either give a single spray (made up of several sprays) or a double spray (for use in 4-valve engines). Typical Sauter mean diameters (SMD) are found to be in the range of 200 μm for multi-hole-type injectors and 300 μm for single-hole-type injectors.

Zhao et al. [2] reviewed published literature on port fuel injection and discussed various types of PFI injectors and their resultant spray structure. The various stages of mixture formation were described, and the important parameters which affect vaporisation and transport processes, namely, fuel properties, injection duration, timing of the injection pulse with respect to the intake valve opening, spray pattern, droplet size distribution, intake port and valve temperatures, targeting accuracy, and manifold pressure, were identified. The characteristics required of a good injector were summarised. The authors also emphasised the need to avoid drawing conclusions from a single parameter such as drop size, and the need to describe and document the entire spray structure. This is especially relevant as most papers in literature are found to give only details of a single global SMD and not other details of the spray.

Kim et al. [3] studied the measurement of spray angles of PFI injectors by three different methods: digital image processing, shadowgraphy, and spray patternation. They observed that the

definition and measurement of the spray angle is difficult due to the curved boundaries of the spray caused by air interaction. The spray angle was found to vary both with time and with axial distance from the injector tip, and with the technique used. Zhao et al. [4] obtained backlit images and PDA measurements on baseline and pressure modulated PFI injectors, and obtained SMD and droplet distribution and velocity data. For the baseline case, the SMD was found to be between 160 and 190 micron for different injectors.

Four different mechanisms of liquid fuel transport into the cylinder were identified by Meyer and Heywood [5]: atomisation, high speed intake air transport, injection contribution, and fuel film squeezing. The effect of various engine and fuel variables on liquid fuel transport into the cylinder was also studied [6]. Phase Doppler Particle Analyser (PDPA) measurements of the spray were also made in a square piston optical engine with a flat cylinder head. The size of droplets entering under open valve injection was found to be smaller than that under closed valve injection, with in-cylinder SMD values in the range of 30 to 90 micron.

Ishii et al. [7] reported SMDs for an air assisted M-jet low-pressure injector to be 120 micron without air assist, and 10 micron with air assist, though details about the location of the measurements are not available. Kato et al. [8] at Yamaha motor company, Japan, studied the influence of PFI parameters on combustion stability by simulating the engine through computational fluid dynamics, and correlating the results with an experimentally determined coefficient of variance (COV) in the net mean effective pressure. They reported measured spray angles of around 5 degrees and SMDs in the range of 120 micron for injectors operating at 3 bar pressure.

Christ and Schlerfer [9] acquired experimental data for a PFI injector using a matrix test rig which could collect droplets from a spray. They also determined droplet velocities and diameters from PDA measurements. No significant changes were observed in the spray at distances of 30 mm, 50 mm, and 70 mm from the injector tip, and it was concluded that secondary breakup is almost nonexistent, with the SMD in the range of 90 to 100 micron. From their experiments, it was also observed that the droplet start velocities are normally distributed around a constant mean value, and are independent of drop size throughout the injection duration. Detailed correlations between droplet sizes and velocities at different locations and times were obtained.

Murakami et al. [10] used CFD as a tool to study the combustion phenomena in a 50-cc engine. The spray was simulated using the Lagrangian-Eulerian method with the Taylor Analogy breakup (TAB) model for secondary breakup. Images of the spray were presented showing the spray penetration. Bianchi et al. [11] studied the effect of injection timing and targeting in a 4-valve motorcycle engine under idling conditions. They used experimental data from the characterisation of the injector under quiescent conditions to initially simulate the spray, and matched the mean diameters and penetration. Using a PDA, they obtained droplet distributions at two locations along the axis for a 3-hole and a 4-hole injector. SMD values were around 120 micron and 100 micron, for the 3-hole and 4-hole injectors, respectively, at 50 mm from the axis, and at 3 ms after the start of the spray. The 4-hole injector showed the highest number density for droplets around 50 micron in size, while the 3-hole injector had the highest number density for droplets of size around 25 micron. The spray angles were between 9 and 11 degrees.

Thus, it is seen that though some studies on PFI sprays have been reported in literature, detailed information, especially time-resolved data on SMD variations, is not available. Also, no satisfactory empirical or analytical correlations are available to predict the spray characteristics for this class of sprays, and hence, experimental investigations are imperative. Further, while high pressure sprays can be simulated accurately by CFD given certain inputs, the same is not true for low-pressure sprays. Low-pressure sprays of the kind studied here differ significantly from high-pressure sprays due to the presence of large ligaments. Consequently, breakup occurs farther away from the injector tip. Most breakup models in literature only deal with the secondary breakup of the spray – it is assumed that the primary breakup is complete and droplets have formed from the sheet/ligaments. Further breakup of these droplets is then simulated. While these assumptions are satisfactory for high-pressure sprays, they do not hold good for low-pressure sprays. Thus, even from an application point of view, comprehensive spray data is very important for low-pressure sprays.

Typically, multiphase flows for engine applications are modelled using a Lagrangian-Eulerian

method: the gas phase is assumed to be a continuous phase, and is solved for in an Eulerian fashion, while the liquid phase is considered to be the dispersed phase, and is solved for in a Lagrangian manner. This approach can be applied to dilute sprays, where the volume fraction of the dispersed phase is small. A PFI engine can be simulated by this methodology if the flow within the injector is not required to be modelled. The exit flow condition of the nozzle is however, required to be known. Models for breakup, collision, coalescence of the droplets, and wall film formation exist, which can be used to model the evolution of the droplets. The 'normal' way is to inject 'blobs' which are of the same size as the injector orifice, and tune these models to match the values from experiments. This is also one of the motivations for obtaining detailed time-resolved measurements. The next few paragraphs describe a brief literature review of the various techniques used to characterise sprays.

Techniques used in literature for droplet size measurements include line of sight diffraction based methods [12] such as a Malvern diffractometer, which though not overly expensive, can however give only average values of droplet diameters. Since the values here are averaged over a volume which corresponds to the path of the laser beam, spatial variations in the spray are lost. The data is, however, useful to obtain a quick idea of the atomization, and is especially useful for comparing the effect of various parameters on dropsizes under production environments.

Phase Doppler Anemometry (PDA), which is widely regarded as the most accurate method, can simultaneously provide droplet sizes and velocities [13]. PDA is essentially a 'point technique' as the measurement volume is generally very small, but the high accuracy and lack of any calibration factors, makes it very attractive for droplet size measurements. The PDA technique however suffers from very high cost due to the need for multiple lasers, and shortcomings in applicability to high pressure sprays and dense sprays.

Laser sheet drop sizing (LSD) which is based on the ratio of planar laser induced fluorescence (PLIF) to Mie scattering, and requires calibration at a point in the spray, is a very attractive technique [14,15]. This method has been applied successfully to very dense sprays such as in those from pressure swirl atomizers [15] and diesel sprays in a running engine [16]. LSD requires utilisation of a dye with similar properties to the fuel, and the concentration of the dye used for fluorescence has to be carefully chosen to minimize errors [17]. Recent findings also suggest that the calibration constant may depend on the diameter of the droplets itself [18]. However, given its ability to give planar information of SMD, and its ability to work under conditions where PDA may fail, LSD is increasingly being seen as an attractive technique. The only drawback is the need for a calibration. This aspect has been addressed in the current work.

Shadowgraphy is the only technique which can be used to characterize droplets and ligaments of arbitrary shapes [19, 20]. However, shadowgraphy can also be utilized only in non-dense sprays since the light illuminates in-focus as well as out-of-focus droplets, as the light rays pass through the entire spray before reaching the camera. Further, more sophisticated image processing is required to differentiate between droplets which are in-focus and those that are defocused, in order to obtain accurate values of droplet sizes [19]. While diffractometers and PDA devices use powerful continuous wave lasers, it is desirable to use pulsed lasers with appropriate attachments which can provide uniform diffuse light for shadowgraphy, or use cameras with very low exposure times such that the droplets are frozen in the images. Granulometry on magnified images obtained from shadowgraphy can then be utilized to obtain droplet size distributions. Long distance microscopes having very small depths of focus are especially useful for such studies.

This paper concerns diagnostics of gasoline sprays from two-hole and four-hole automotive PFI injectors. A combination of techniques, i.e., Mie scattering and LSD has been used to obtain quantitative information about the sprays. The following sections provide a detailed description of the experimental setup and data on the spray structure, cone angle, spray tip penetration, and droplet velocities. Temporal variation in SMD values from granulometry are then presented and discussed. The LSD technique is then described, and calibrated LSD images showing SMD values in a plane at different instants of time are presented and discussed. Finally, the results of the paper are summarised.

2. EXPERIMENTAL SETUP

Experiments were carried out on a PFI facility which consists of a low pressure injector with a fuel

pump arrangement which maintains the pressure at 2.4 bar. A modified two-wheeler fuel tank houses the pump which is powered by a 12 V, 1 A power supply. The pump gives a fuel flow rate of 14.7 g/s as indicated by a mass flow meter in the line. A pressure sensor in the line reads the line pressure, while a one-way pressure relief valve ensures that pressure downstream is constant at 2.4 bar. The excess fuel is fed back to the tank. LCD panels show readouts of the pressure, flow rate, and number of times the injector is fired. An emergency stop switch and circuit breakers which activate on the improper working of the pump or injector ensure a high level of safety. The injector is actuated by means of an electronic circuit. The fuelling duration and frequency can be modified by means of a signal generator. A square pulse of 10 V amplitude is fed from the signal generator, which causes the opening of the injector's solenoid valve. This signal is amplified by a power circuit to account for the amperage required, and fed to the injector. A square Perspex collecting chamber (10 x 10 x 20 cm) was fabricated to collect the spray and the rig was placed under an exhaust duct in order to remove any fuel vapours. Various experiments were carried out on the injector. The frequency of firing was maintained at 1 Hz, since at higher frequencies, a few droplets from the previous injections were found to linger in the Perspex chamber. The pulse width corresponding to the injector firing duration was maintained at 8 ms, which corresponds to the firing duration under real engine conditions of high load and speed.

The experimental setup for experiments on the PFI facility includes laser, optics, cameras and synchronisation equipment. A schematic of the experimental setup is shown in Fig. 1, and a brief description of the various components is given below.

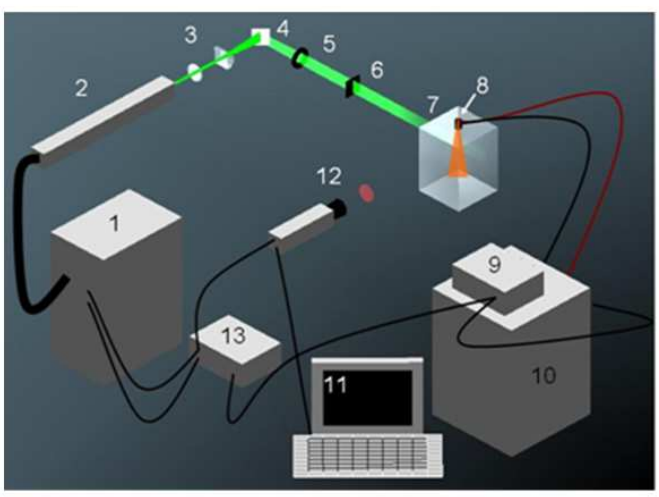

1. Laser power and cooling
2. Laser head
3. Lenses
4. Mirror
5. Aperture
6. Slit
7. Perspex chamber
8. Injector
9. Function generator
10. Fuel pump and power supply
11. Data acquisition computer
12. Camera with filter
13. Delay generator

Figure 1: Schematic showing the setup for the laser diagnostics experiments.

2.1 Lasers

Three lasers were used as light sources for the work done in this paper: A 300 mW continuous-wave green diode laser with a wavelength of 532 nm (Manufacturer: Roithner) was used wherever a continuous light source was required - for example, in conjunction with high speed cameras. A 50 mJ double-pulsed Quantel Nd:YAG laser was used for velocity measurements. This laser was used as a source of green light (532 nm), and has a repetition rate of upto 15 double-pulses per second. The time between the two pulses was varied by using a delay generator. A single-pulsed Quantel Brilliant Nd:YAG laser (400 mJ at 1064 nm) was used for most of the experiments. A doubling crystal was used to generate a green beam (532 nm) with the energy being 180 mJ for a 5 ns pulse. The laser fires at 10 Hz while running in its internal mode. Whenever synchronisation was required, the laser was run with both the flashlamp and the Q-switch triggered externally.

2.2 Optics

Optical hardware was used both to align and steer the beam, and to increase the optical path to make synchronisation possible. The beam from the laser, which has a circular cross section, was made into a plane by passing it through convex and cylindrical lenses. A cylindrical lens with a focal length of 50 mm was used to create the planar sheet. The beam was turned through a right angle using a front-coated mirror (80 x 80 mm) to avoid multiple reflections. An iris was used to limit the height of the beam. A cylindrical lens having a long focal length (300 mm) or a slit was used to reduce the width of the laser sheet. The optics were held in posts mounted on stages to allow fine movement. These in turn, were mounted on an optic table.

2.3 Cameras

Three different cameras were used according to the phenomenon studied. A Phantom 6 camera capable of taking upto 250000 frames per second was used for high speed imaging. A Sharpvision CCD camera capable of taking upto 12 sets of 2 images per second was used to acquire images in conjunction with the double-pulsed laser. This camera has a minimum exposure time of 40 μs, and a pixel array of 1360 x 1036. Due to its high resolution, this camera was also used where magnification was important, e.g., where magnified images of small parts of the spray were required to be acquired. An Intensified Charge Coupled Device (ICCD) camera was used where a large dynamic range and low noise was required: for PLIF. This camera (Manufacturer: Stanford Computer Optics) has a resolution of 648 x 484 pixels, and a minimum exposure time of 1 ns. It is capable of taking upto 60 images per second. The very low exposure time capability helps in reducing noise to a large extent and weak intensities of fluorescence can be effectively captured.

2.4 Synchronisation Equipment

Signal generators and delay generators were used to synchronise various events such as the start of injection, laser firing, which is a nanosecond event, and camera triggering. Square pulses from a master signal generator were used to operate the injector. To acquire images at different points of time after the start of the spray, the master signal was delayed by known intervals and fed to the camera. Suitably delayed inputs were fed to the flash lamp and Q-switch of the laser to operate them with the least possible jitter. Using the above arrangement, an exposure time of 60 ns was sufficient to capture images, when using the ICCD camera. A Tektronix oscilloscope, capable of acquiring 2 gigasamples per second, was used to monitor the signals. The timing diagram used is shown in Fig. 2.

Various techniques were used to obtain the different spray parameters: Microscopy for the nozzle orifice diameters, Mie scattering to measure spray tip penetrations and cone angles, and Laser Sheet Dropsizing (LSD) for the Sauter mean diameter (SMD). The techniques and results are discussed in the following sections.

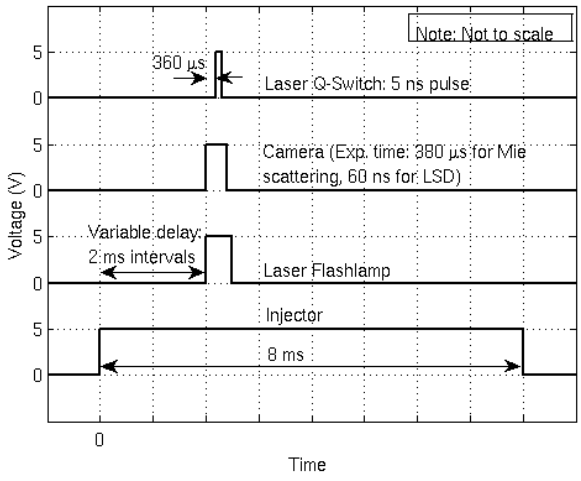

Figure 2: Timing diagram showing the synchronised signals for Mie scattering and PLIF experiments (for the spray structure, granulometry, and LSD).

Figure 3: A PFI injector.

2.5 PFI injectors

Figure 3 shows a photograph of the two-hole PFI injector. It is a low-pressure, plate type, solenoid operated injector. Two injectors were studied - one with two orifices, and the second with four orifices. Images of the injectors were acquired with a reflective-type light microscope to find the nozzle orifice diameters. These were obtained using a Zeiss microscope operated with the Axio Vision acquisition software. Figure 4 shows microscopy images of the plate surface of the 2-hole and 4-hole injectors. The details of the orifices are seen here - the two orifices are approximately 270 micron in size and 730 micron apart for the 2-hole injector. In the 4-hole injector, the orifices are approximately 190 micron in size and their centres are in a circle of diameter 920 μm. Being plate type injectors, the spray from these injectors is expected to be a 'pencil type' spray with a low divergence angle [1].

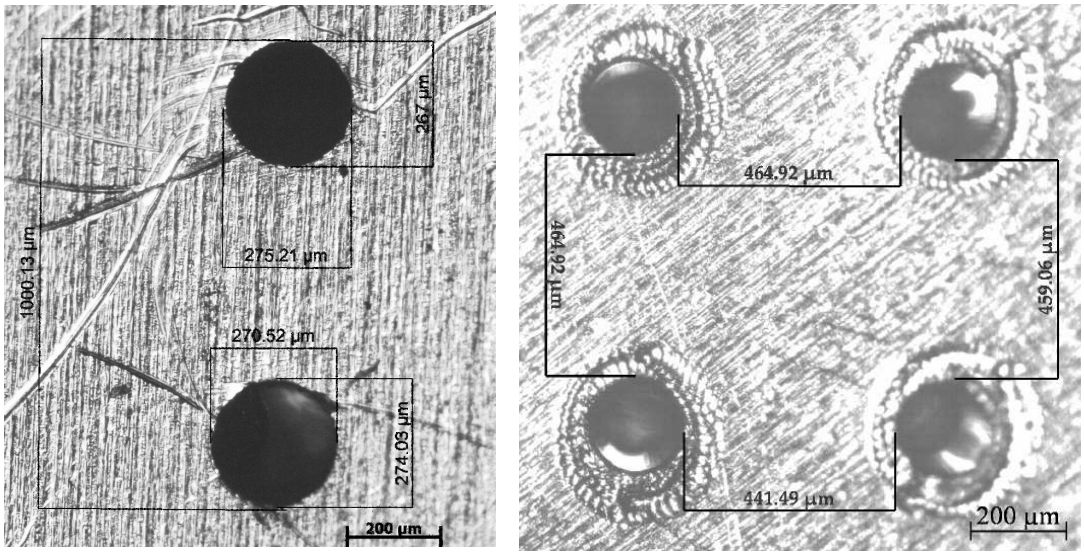

Figure 4: Details of the 2-hole and 4-hole injector plates.

3. RESULTS AND DISCUSSION

3.1 Spray development, spray cone angle and spray tip penetration

Preliminary experiments were required to obtain a basic idea of the spray structure since no prior data were available. A laser sheet was formed using the optics described earlier, from the continuous wave 300 mW, 532 nm diode laser. This sheet was passed through the spray and the spray was photographed using two different cameras: a Kodak Motioncorder camera at 1000 frames per second, and a Phantom 6 camera at speeds upto around 50000 fps. While the images from these cameras give an idea of the time evolution of a single spray, the data were not very useful for determining droplet sizes since there was blurring of images owing to the low resolution of the images particularly at high speeds and the large exposure times: at lower exposure times, the signal in the images was very low as the light intensity available from the continuous-wave diode laser was insufficient. However, it was observed from the data that large ligaments were present. This is to be expected since the injection pressure is very low. The images indicated that the length required for breakup is substantial. This is also observed in Figs. 5 and 6.

As mentioned earlier, very few papers with quantitative time-resolved data on low-pressure PFI sprays are to be found in literature. Spray structures observed in this study are however, similar to the qualitative images seen in previous studies [1]. It is observed that a considerable portion of the spray near the injector is not atomized. One of the challenging aspects of droplet measurements in such sprays is that a large number of droplets may not be spherical. This aspect is important for spray techniques, as many commonly used methods assume the droplets present to be spherical.

The spray cone angle and penetration were obtained from Mie scattering images of the full spray. Images numbering 300 with the laser sheet passing through the mid-plane of the spray were acquired with a Sharpvision camera mounted with a 25 mm Pentax quartz lens. The 532 nm green beam from the 10 Hz Nd:YAG laser was used for these experiments. The images were ensemble-averaged after subtracting the background (to eliminate electronic noise and ambient light). Since the spray from a low pressure injector does not have a constant well-defined cone angle as in the case of high pressure sprays, the angles here were taken with reference to a downstream point at a distance equal to 60 times the diameter of the orifice [21]. The cone angle in such low-pressure sprays is difficult to estimate near the injector due to the presence of ligaments which lead to a delayed breakup. Hence, the spray cone angle in other studies has been found to be often determined by mechanical methods such as collecting the spray using a patternator, and then determining the mass at different locations [22].

Figures 5 to 8 show instantaneous and averaged images of the spray, 8 ms after the start of injection. Figure 5 shows the instantaneous Mie-scattering with the laser sheet passing through only 1 orifice, and perpendicular to the plane passing through both orifices. Figure 6 shows the Mie-scattering image when the laser sheet is aligned with the centres of both orifices of the injector. In other words, the plane of image in Fig. 5 is perpendicular to that in Fig. 6. The corresponding ensembled images are shown in Figs. 7 and 8, respectively. It is observed that though the instantaneous images show a wide spread of droplets, due to variations from spray-to-spray and presence of ligaments in the core region, the ensemble images resemble a ‘pencil spray’ as predicted by Lenz [1]. The breakup process is extremely complex with the interaction of the jets from the 2 or 4 nozzle holes. It is possible that the interaction between the jets leads to a reduction in the breakup length – the breakup length is shorter in the case of the 4-hole injector (The effect of the smaller hole size in the 4-hole injector cannot be discounted though). It is likely that a single hole injector would have a longer breakup length for the same mass flow rate. The breakup length is important from an engine application perspective since the nozzle would have to be located such that any regions of impingement would be beyond the breakup length.

The spray half-cone angles from the processed images at various points of time were found to be between 4 and 8° for the 2-hole injector. The injector was tested in two orientations - with the laser sheet passing through one orifice of the injector, and with the laser sheet passing through both orifices of the injector. The spray half-cone angle at different points of time was found to be similar in both cases. The spray cone angle was found to be better defined in the 4-hole injector and around 7°. The angle was found to be retained far away from the injector tip also. A smaller presence of ligaments due to the smaller orifice size could explain this.

The spray was photographed at 1 ms intervals from the start of the injection pulse and ensemble averaged images were obtained. The location of the spray tip was found from these images. Figure 9 shows the evolution of the spray with time, and Fig. 10 shows the variation of the spray tip penetration. The slope of the spray tip penetration curve gives an approximate estimate of the droplet velocity in the spray tip region, which was found to be around 20 m/s. This estimate was refined by particle tracking velocimetry measurements. While the injection velocity could not be directly measured at the nozzle tip due to the presence of ligaments, it could be measured at 20 mm from the nozzle tip. Using the setup described earlier, and with the camera in PIV mode, 2 successive images of the spray were taken, 20 μs apart. Due to the low number of droplets and the large droplet sizes, the images could not be processed with standard PIV software. A particle tracking velocimetry approach was adopted: individual droplets were identified in both images and their displacement calculated. Their velocity was then determined, knowing the time separation between the image pairs. The velocity of the larger droplets (which are relatively unaffected by the drag force due to air) was estimated to be 20.5 m/s at 20 mm from the injector tip.

From the Mie images of the spray, a lag of 1.3 ms was observed to exist between the transmission of the electronic pulse for injection and the emergence of fuel from the injector. Similarly, though the electronic injection pulse was stopped at 8 ms, fuel was found to be injected upto 11 ms.

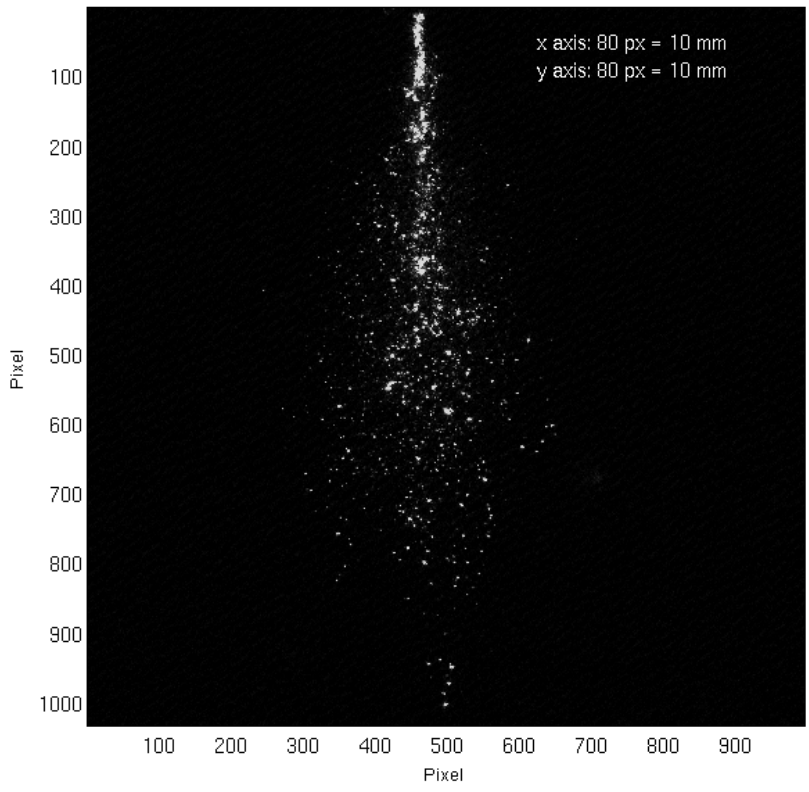

Figure 5: Instantaneous Mie scattering image of the spray at 8 ms (laser sheet through 1 orifice).

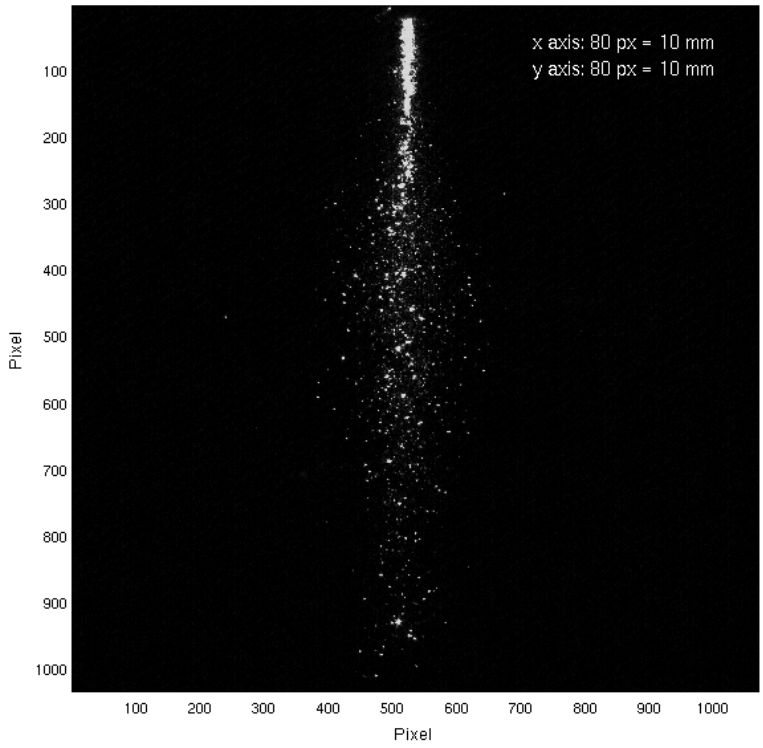

Figure 6: Instantaneous Mie scattering image of the spray at 8 ms (laser sheet through both orifices).

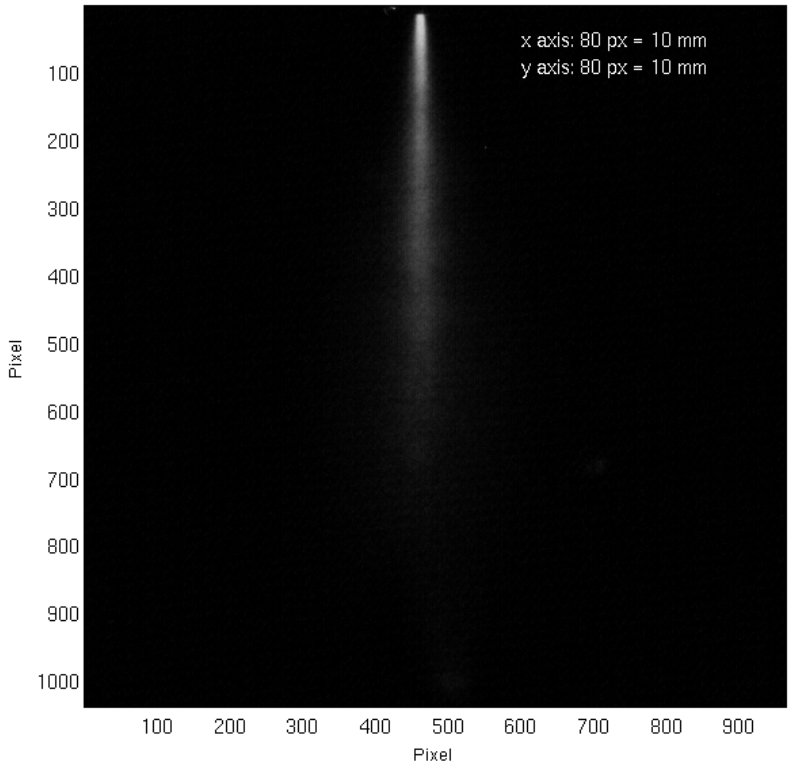

Figure 7: Averaged Mie scattering image of the spray at 8 ms (laser sheet through 1 orifice).

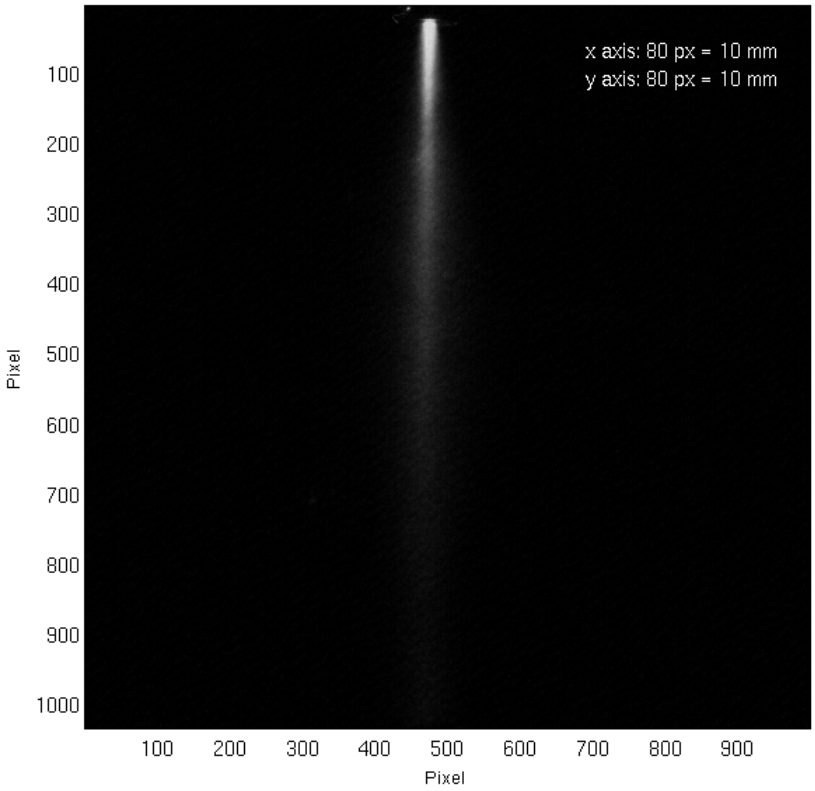

Figure 8: Averaged Mie scattering image of the spray at 8 ms (laser sheet through both orifices).

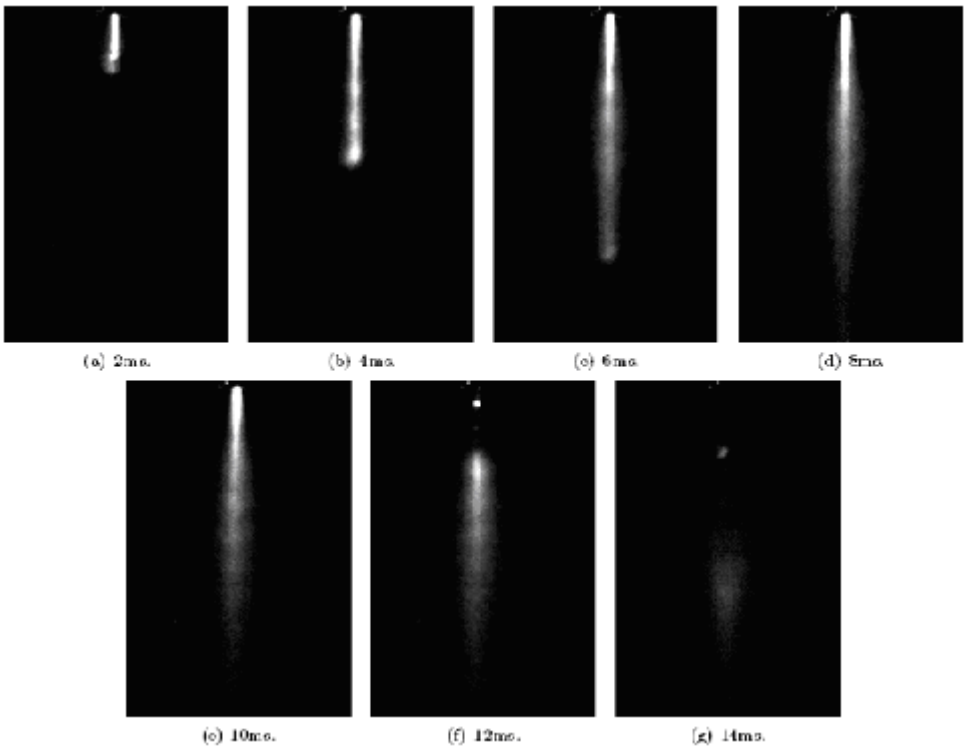

Figure 9: Evolution of the spray: Processed images at 2 ms intervals.

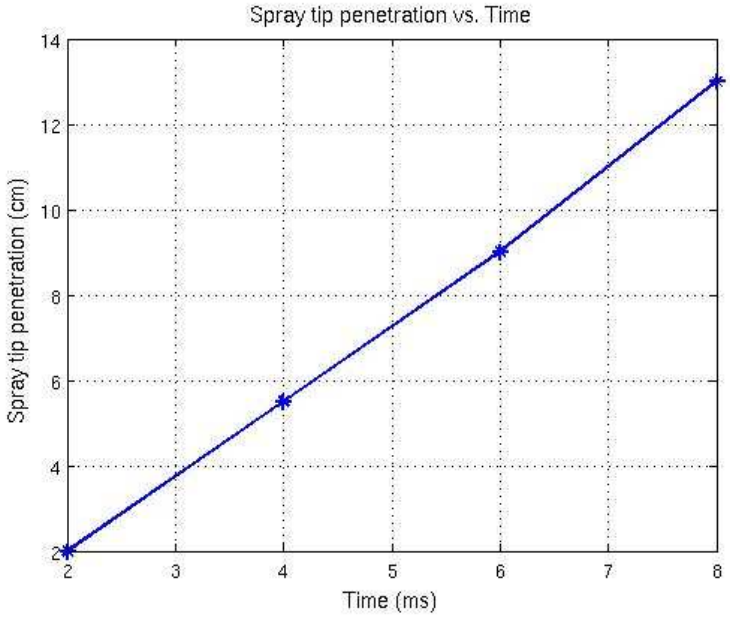

Figure 10: Variation of spray tip penetration with time.

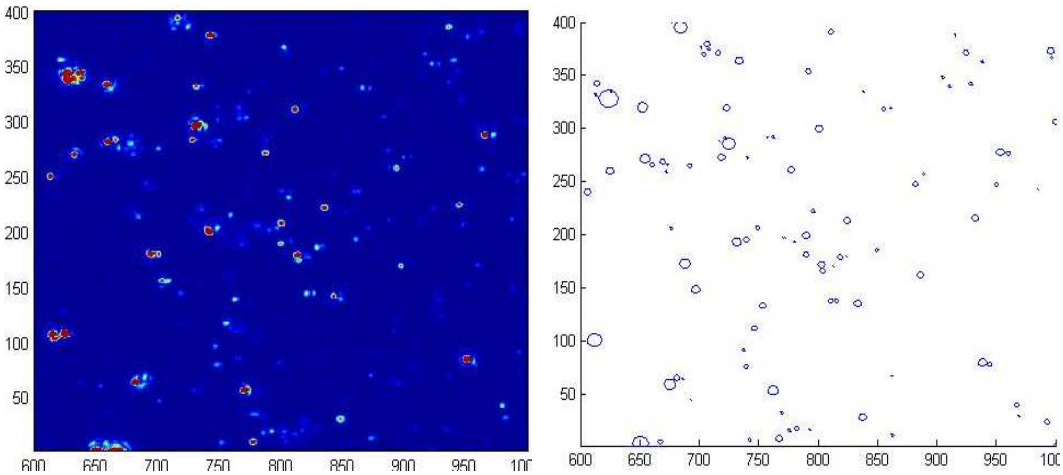

Figure 11: Typical raw (false colour) and processed images showing droplets at 45 mm from the injector tip.

3.2 Granulometry

Droplet sizes and distributions were obtained by granulometry. Direct imaging of the spray was performed at a high magnification. The spray was illuminated by the pulsed laser, operating at 532 nm. Cylindrical and spherical lenses were used to create a laser sheet which was passed through an axial plane of the spray.

A signal generator was used to create a square pulse with a duration of 8 ms. This pulse was fed to the injector through an amplifying circuit. The delay generator was used to synchronise and trigger both the laser and camera. The laser was fired with both the flash lamp and Q-switch in external mode. A delay of 360 μs was set between the flash lamp and laser firing to reduce the intensity of the beam (as against a delay of 200 μs for maximum power).

The Sharpvision CCD camera used has a chip area of 1360 x 1036 pixels, with an 8 bit resolution. An exposure time of 380 μs was used for these experiments. A Sigma 70-300 mm lens was used in macro mode to focus on a small region (13 mm wide x 10 mm high) of the spray. Using a calibration target, the number of pixels per mm was found, and hence the pixel size was found to be ~10 micron for the given configuration.

Images of the spray were acquired at three axial locations corresponding to 45 mm, 75 mm, and 105 mm below the injector tip, an example of which is shown in Fig. 11. Both the laser and camera were triggered at various times (2 ms intervals) after the electronic pulse was given to the injector. The images were acquired to a PC connected to the camera by a firewire port. The images were processed as described below: First, images of the background noise and Rayleigh scattering of the laser light by the air were obtained. After subtracting the background, the images were processed using the Ximager software [23]. This involved specifying a threshold so that the software could clearly distinguish droplets from the background. A lower cut-off of 20 on the intensity scale was chosen after a study of the effects of various thresholds. High thresholds lead to large reductions in the droplet areas, and artificially lower droplet sizes - often the software treats the two glare points of the drop as separate droplets, while low thresholds cause inclusion of background noise as droplets. The granulometry module of the software was then used to process and summarise the images: the x and y locations of all the droplets identified in an image, and their respective areas in pixels, were recorded for further processing in Matlab. The change in the SMD value based on threshold was found to be less than 10% (less than 5% in many cases) when the threshold was varied from 10 to 20.

The droplets were then assumed to be spherical (circular in cross section), and their diameters and volumes calculated. This process was repeated for each of the droplets in all 300 images. The sum of the volumes of the droplets was divided by the sum of the areas to get the SMD. This procedure was performed for sets of images at each of the three locations, at different times. Comparisons with SMD values from 200 images did not show significant differences in SMD, (a difference of about 1%) thus showing that the number of droplets sampled in the images is statistically large enough.

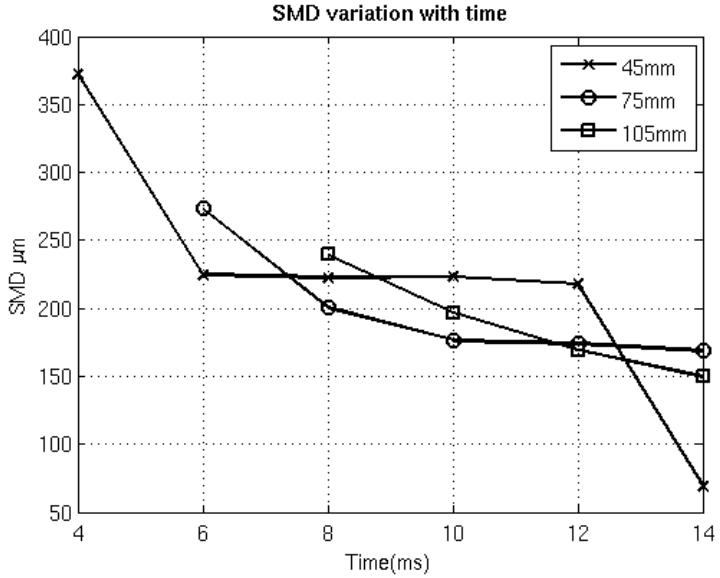

Figure 12: Variation of SMD with time at different locations for the 2-hole injector.

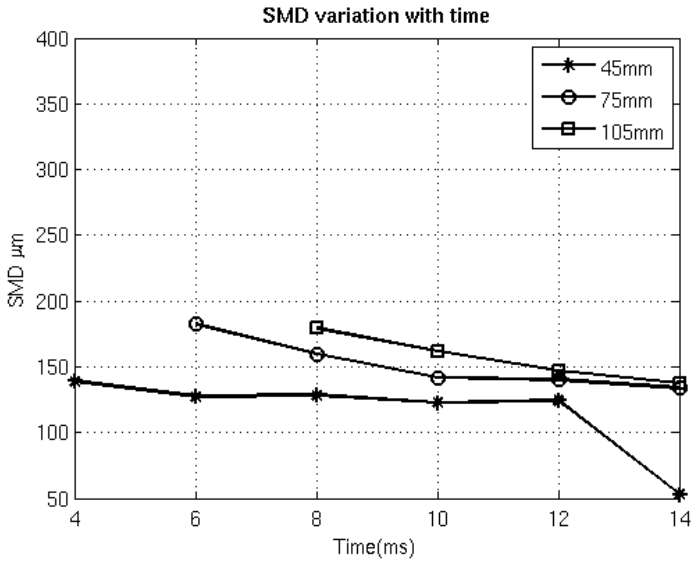

Figure 13: Variation of SMD with time at different locations for the 4-hole injector.

The variations of SMD with time for the 2-hole injector, at the 3 different locations, are shown in Fig. 12. At each of the locations, it is seen that the SMD is initially high (which corresponds to large droplets entering the viewing section), followed by a nearly constant region corresponding to steady flow from the injector. This is followed by a low SMD. At a section 45 mm from the tip of the nozzle (in Fig. 12), the SMD drops sharply from 364 μm at 4 ms to 220 μm at 6 ms, after which it remains fairly constant upto 12 ms. This initial high value is also probably due to the injection of large droplets at the start of injection. During the bulk of the injection, the injection rate and hence the SMD remain constant. Later, while the injection tapers off around 12 ms, the SMD also drops. This could be both due to the smaller mass of fuel injected towards the end, and due to the fact that while the larger droplets fall rapidly, the smaller droplets drift in the air longer, leading to a smaller SMD.

A similar trend is observed at the 75 mm and 105 mm locations with the initial SMD being higher and then falling, but the further drop in SMD at these locations is not seen due to the unavailability of data at times beyond 14 ms. Results for the 4-hole injector are similar to those obtained for the 2-hole injector, and are shown in Fig. 13. It is of interest to note that a decrease in the individual orifice size from 270 to 190 μm has caused a large difference in the SMD of the spray initially. However, at later times, the difference in the SMD of the spray from the two injectors is not as large. The trends in the variation of SMD are similar at the three axial locations. However, from 8 to 12 ms, the values of SMD far away from the injector tip are about 20 % higher than those at 45 mm from the injector tip. It is possible that the SMD values at the centreline far away from the injector could be higher due to the dispersion of smaller droplets, for the 4-hole injector. Another reason could be that the smaller droplets produced initially from this nozzle coalesce to form larger droplets which are reflected in the increase in SMD. This is because there is a high incidence of droplet collisions at the centreline due to the interaction of the individual jets from the four holes. It is interesting to note that computational fluid dynamic simulations of such sprays utilising collision models based on empirical data yield inaccurate results such as predictions of large, sudden changes in the SMD. This was observed in simulations which were performed using the experimentally-obtained diameter distribution at 45 mm from the injector tip as an input. The simulations were performed using the AVL FIRE code, for the same conditions as the experiments: PFI spray from a 2.4 bar injector in quiescent air. The Taylor analogy breakup (TAB) model [24] with standard constants for secondary breakup, and coalescence and collision model of O'Rourke et al. [25] were used in this simulation. The predicted results showed large variations in the SMD, The experimental results, however, show SMD values along the axis to lie in a relatively small range (Fig. 12), which is in agreement with trends observed by other researchers [9]. Thus, it is possible that coalescence in these low-pressure sprays is either low or

that the models which were proposed initially for high pressure sprays are not accurate for this class of sprays. The collision and coalescence phenomena in such sprays merit further study, and these need to be revisited for low-pressure sprays.

Sample droplet distributions by number density and volume for the 2-hole injector are shown in Figs. 14 and 15. It is seen that small droplets (<100 μm) are large in number, while the larger droplets, (>100 μm) though few in number, still contribute to a large part of the spray by volume.

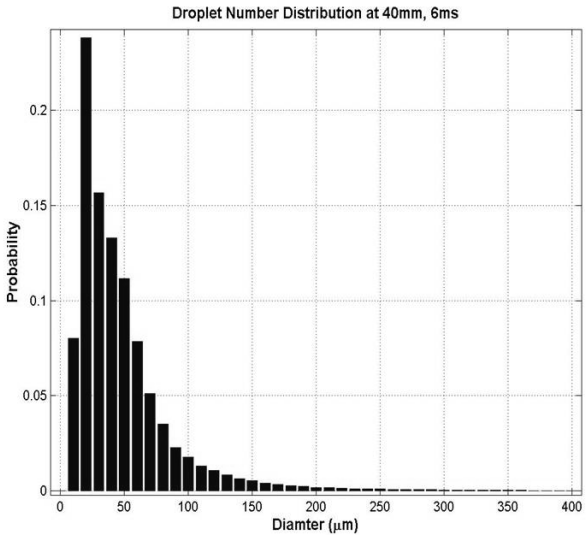

Figure 14: Droplet distributions for the 2-hole injector by number density at 45 mm from the injector tip, 6 ms after the start of the spray.

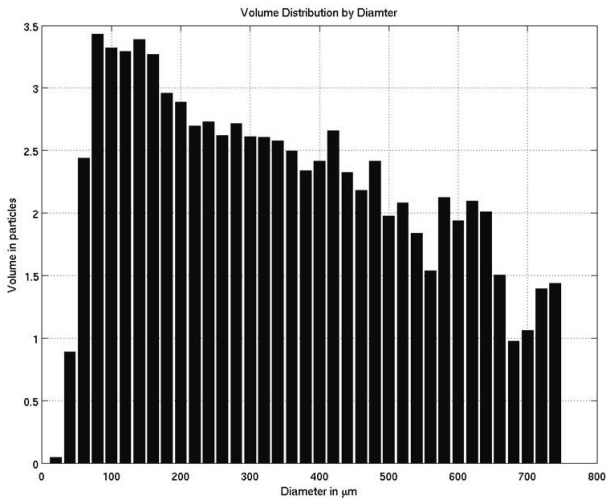

Figure 15: Droplet distributions for the 2-hole injector by volume at 45 mm from the injector tip, 6 ms after the start of the spray.

3.3. Laser Sheet Dropsizing (LSD)

Laser Sheet Dropsizing (LSD) or Planar Droplet Sizing (PDS) is a technique which can be used to obtain simultaneous spatial distribution of droplets, and liquid volume and concentration [17]. The formulation and application of the technique from literature [13-18, 26] is summarised below. The method has also been used with water sprays [27] and in diesel engine [16] and gasoline direct injection conditions [14]. Among the benefits of LSD is that it is a planar method, and hence, is less time consuming. The equipment required is also less expensive than the PDA setup.

The technique itself involves using images of:

- Mie scattering, and
- Planar laser induced fluorescence (PLIF)

Since the intensity of the Mie scattering is proportional to the area of the droplet, and the intensity of PLIF is proportional to the volume, if images of the Mie scattering and fluorescence of the same setup are acquired with the same set of optics and camera and the intensities are divided, the equations yield,

$$I_{LIF}/I_{MIE} \alpha D_{32} \quad (1)$$

$$D_{32}=k\, I_{LIF}/I_{MIE} \quad (2)$$

where D_{32} is the ratio of volume to the area of the droplets, i.e., the SMD. If the proportionality constant can be determined by some method, the Sauter mean diameter at different locations in the spray can be obtained from LSD. One method for calibration is to use a mono-disperse droplet generator and use exactly the same experimental conditions (laser power, aperture, intensification, focal length, and distance) as in the actual experiments. This is difficult to ensure, and hence other methods are followed. For the present study, quantitative data obtained by applying the granulometry method on the magnified Mie-scattering images of small portions of the spray were used to calibrate the LSD images. To the best of our knowledge, this is the first work wherein granulometry based data has been used to quantify LSD images in a PFI spray. This method had the added advantage that no separate equipment was required to calibrate the spray.

3.4 LSD Experiments

The experimental setup for the LSD measurements consists of the PFI facility, pulsed laser, fused silica lenses and a fluorescence filter. In the present study, the spray can be considered non-evaporating in the time scale of the experiment (lifetime of a 20 micron droplet is around 40 ms as computed by the D^2 law), and hence Rhodamine-6G, which is a non-evaporating dye, could be used as the fluorescence tracer. **Error! Reference source not found.**This dye can be excited in the visible range (Laser radiation at 532 nm) and its emission is centred at 590 nm. Images (Mie scattering and PLIF) were acquired at 2 ms intervals using the ICCD camera. For capturing the fluorescence, an Edmund optics broad band filter centered at 600 nm with a FWHM of 80 nm was used. Gasoline with no dye was sprayed and it was confirmed that the Mie scattering was not passing through the filter. Subsequently, 0.02 g of Rhodamine 6G was dissolved in 200 ml of ethanol. This solution was mixed with 4 litres of gasoline and used for the experiments. The concentration of Rhodamine used (5 mg/L of gasoline) was chosen as the lowest value from literature.

Around 300 images at each time setting were acquired and ensemble-averaged after subtracting the background to get the final image of the Mie and Fluorescence. All the images were acquired with a gamma of 1, and care was taken to ensure that there was no saturation of intensity at the pixels. The LSD images were calibrated by using the data from the granulometry images. A region of 1 mm x 1 mm corresponding to 300 x 300 pixels in the granulometry images was taken as the reference section, and the SMD was calculated using the method previously described. As the region chosen corresponds to 3 x 3 pixels in the LSD images, the images were processed, averaging over 3 x 3 pixels. The images were then calibrated at a point, using granulometry data. An average calibration constant was determined using the granulometry data at 3 different sections 45 mm, 75 mm, and 105 mm from the injector tip, with a standard deviation of 33% from the average. The main source of this variation is the dependence of PLIF intensity on diameter. There can be deviations from the ideal dependence of PLIF signal which is d^3. This index depends on the dye concentration [17]**Error! Reference source not found.**, and is not known for the present configuration. The real dependence in future studies can be determined by looking at the PLIF intensities from monodisperse sprays from a droplet generator, and the dye concentration suitably chosen.

Figures 16 and 17 show the calibrated images of the spray in the axial plane, at 8 ms and 12 ms after the start of the injection pulse respectively, for the 2-hole injector. It is seen that the SMD is highest at the lower parts of the spray (at larger distances from the tip of the injector). This trend was also noticed from the granulometry images. Images at earlier times have not been presented

here as similar trends are observed. The images also show that the SMD is higher at the centreline, with smaller droplets being found at the edges at the spray (as was seen in the Mie scattering images of the spray shown earlier). The figures suggest that the larger droplets, which contain most of the fuel injected, have low radial velocity components, and travel along the axial (downward) direction. This may be causing air entrainment along the centreline and the consequent pressure drop due to higher air velocities. It is possible that the smaller droplets which remain nearby get drawn towards the centre of the spray. This may be causing the particular shape of the spray seen in Fig. 16, which is quite different from that observed in high pressure sprays.

Figures 18 and 19 show the calibrated images of the spray at 8 ms and 12 ms after the start of the injection pulse respectively, for the 4-hole injector. Similar trends to that of the 2-hole injector spray are seen, with the diameter being highest far away from the nozzle. However, while the jets from the 2 holes cannot be distinguished in the case of the 2-hole injector, in case of the 4-hole injector, the sprays from the 4 orifices form distinct regions which are also visible in the LSD images.

It is worth emphasising here that though the uncertainty in the dependence of PLIF on diameter introduces some uncertainty in the calibration factor and consequently in the SMD, LSD is a quantitative technique, and as such, the LSD images give the numerical value of SMD at any point in the spray. For the standard deviation of the mean reported earlier, the error bar on these measurements based on a 95% confidence level is ±20%. However, at parts close to the tip of the injector, the assumption of the dependence of PLIF on diameter is violated due to the presence of ligaments, and hence the data is not expected to be accurate in that region. This is, in fact, a limitation of all techniques found in literature.

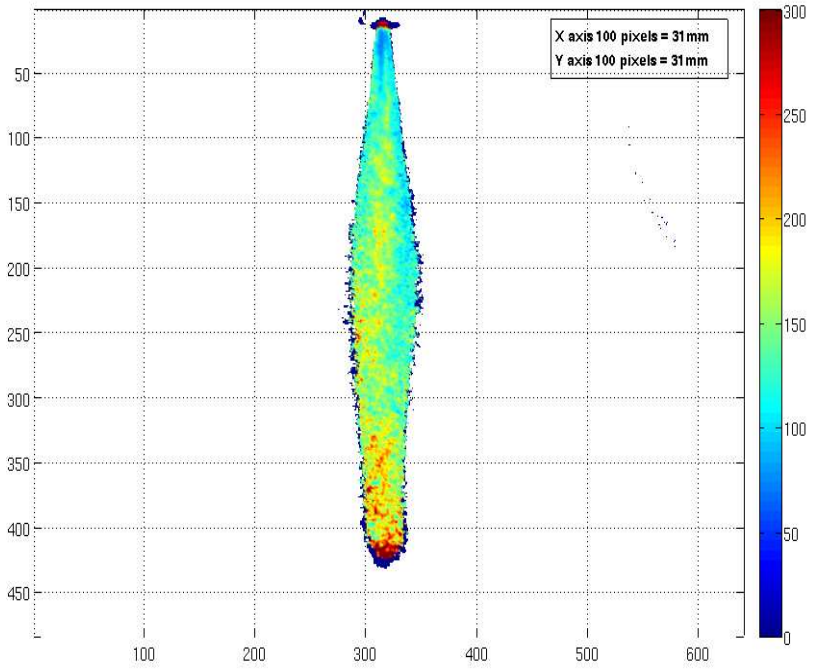

Figure 16: LSD: calibrated image of the spray from the 2-hole injector at 8 ms. The colourbar indicates the magnitude of SMD in μm.

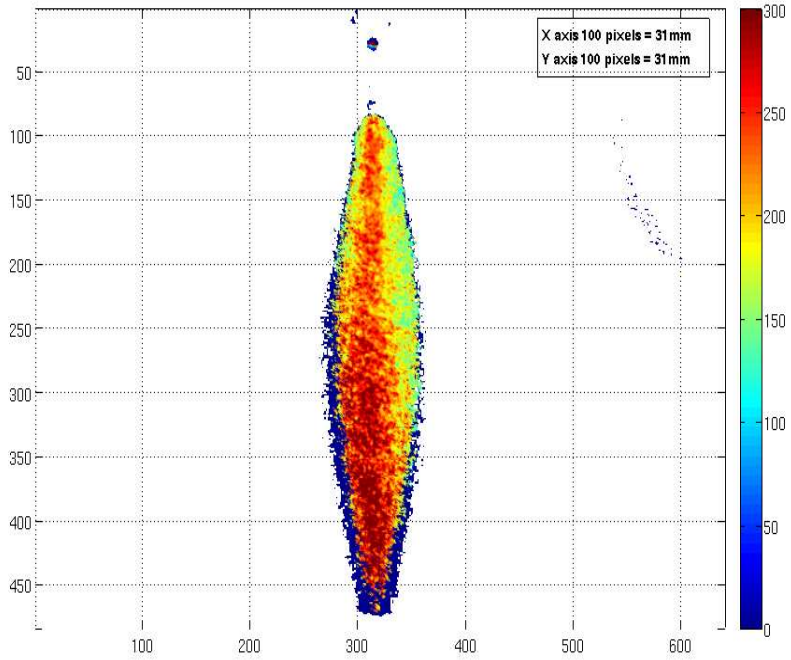

Figure 17: LSD: calibrated image of the spray from the 2-hole injector at 12 ms. The colourbar indicates the magnitude of SMD in μm.

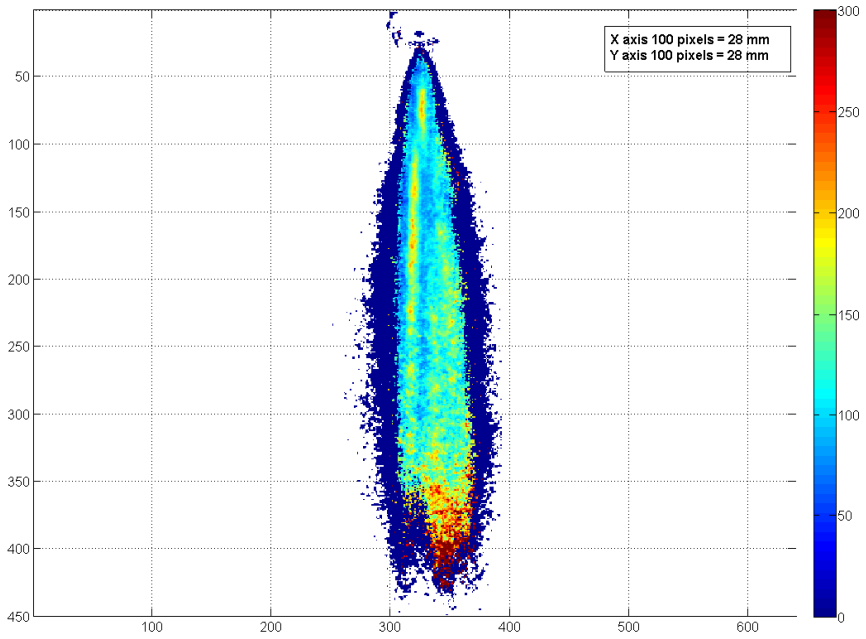

Figure 18: LSD: calibrated image of the spray from the 4-hole injector at 8 ms. The colourbar indicates the magnitude of SMD in μm.

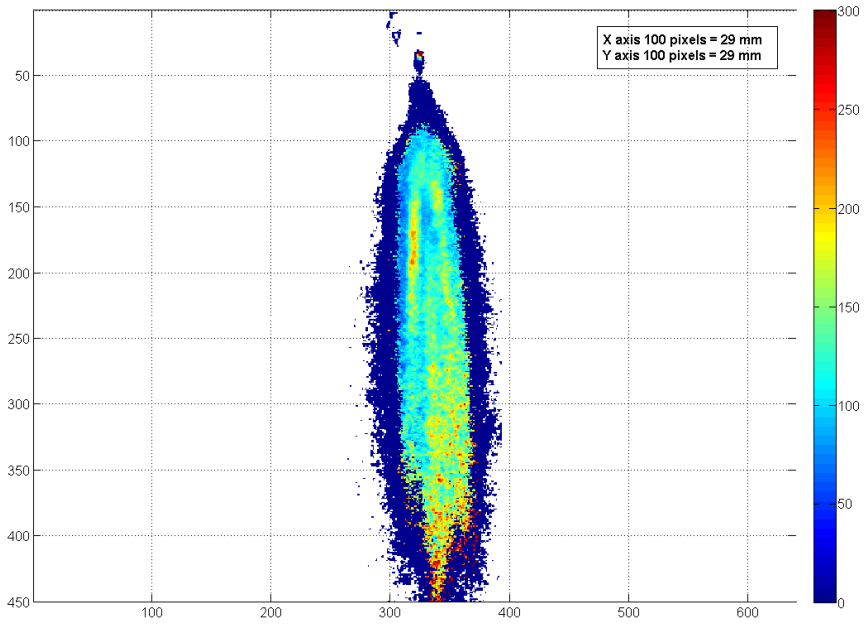

Figure 19: LSD: calibrated image of the spray from the 4-hole injector at 12 ms. The colourbar indicates the magnitude of SMD in μm.

4. CONCLUSIONS

Several laser-based diagnostic techniques have been applied to sprays from 2-hole and 4-hole plate-type PFI injectors. This is, to the best of our knowledge, the first reported study describing the detailed spatio-temporal SMD distribution of low-pressure PFI gasoline sprays. Also, a novel method of calibrating LSD images of Sauter mean diameter using granulometry is reported. The objective was to generate time-resolved quantitative data on these low-pressure sprays in terms of the structure, penetration, and drop-sizes. A comprehensive study of the spray has been done with state-of-the-art techniques, with all the important parameters such as the spray angle, spray tip penetration, mass injected, droplet velocities, droplet distributions and SMDs, being measured. The spray was observed to be pencil-like with a low spread, and breakup lengths of several centimetres. The mass of fuel injected was found to be 12 mg per 8 ms pulse. Spray droplet size distributions were determined at three different locations along the axis of the spray at 2 ms intervals in time, and found to be in the range of 200-250 micron for the 2-hole injector and around 120 micron for the 4-hole injector. Thus, a large reduction in the SMD was observed when going from the two-hole to the four-hole injector. The variations of SMD with time and space were also determined. At the axial locations, the SMD was found to be initially high, followed by a near constant value after which it drops. The spray half cone angle was found to be around 6° for 2 and 4 hole injectors, and the injection velocity was found to be around 21 m/s. Using LSD technique, two-dimensional SMD contours for the entire spray in a central plane were determined with reasonable accuracy (±20%). Lastly, such detailed data of the spray structure would be extremely useful as an input in a Computational Fluid Dynamics (CFD) simulation of PFI engine processes.

ACKNOWLEDGEMENTS

The authors are grateful to Prof R. I. Sujith of IIT Madras, for the Ximager software which was used to process images for granulometry in this work.

REFERENCES

[1] Lenz H. P., Mixture Formation in Spark-Ignition Engines, *Springer-Verlag/Wien*, 1992.

[2] Zhao F. Q., Lai M. C. and Harrington D. L., The spray characteristics of automotive port fuel injection – a critical review, *SAE Paper 950506*, 1995.

[3] Kim Y., Lim J. and Min K., A study of the dimethyl ether spray characteristics and ignition delay, *IJER*, vol. 8, n. 4, pp. 337–346, 2007.

[4] Zhao F. Q.,Amer A. A., Lai M. C. And Dressler J. L. "The effect of fuel-line pressure perturbation on the spray characteristics of automotive port fuel injectors", *SAE Paper* 952486, 1995.

[5] Meyer R. and Heywood J. B., "Liquid fuel transport mechanisms into the cylinder of a firing port-injected SI engine during start up", *SAE Paper* 970865, 1997.

[6] Meyer R. and Heywood J. B., "Effect of engine and fuel variables on liquid fuel transport into the cylinder in port-injected SI engines", *SAE Paper* 1999-01-0563, 1999.

[7] Ishii W., Hanajima T. and Tsuzuku H., "Application of Air-Fuel Mixture Injection to Lean-Burn engines for Small Motorcycles", SAE Paper 2004-32-0052, 2004.

[8] Kato S., Hayashida T. and Iida M., "The influence of port fuel injection on combustion of a small displacement engine for motorcycle", *SAE Paper* 2007-32-0009, 2007.

[9] Christ A. and Schlerfer J., "Spray simulation for low pressure port fuel injectors", *Eighth International Conference on Liquid Atomization and Spray Systems*, pp. –, July 2000.

[10] Murakami Y., Kurosaka H. and Kamiya H., "Practical Application of Combustion Simulation using CFD for Small Engine of Two-Wheeled Vehicle", *SAE Paper* 2004-32-0006, 2004.

[11] Bianchi G. M., Brusiani F., Postrioti L., Grimaldi C. N., Marcacci M. And Carmignani L., "CFD analysis of injection timing and injector geometry influences on mixture preparation at idle in a PFI motorcycle engine", SAE Paper 2007-24-0041, 2007.

[12] Zhao H. and Ladammatos N., "In-Cylinder liquid fuel measurement", *Engine Combustion Instrumentation and Diagnostics*, pp. 395–450, SAE International, 2001.

[13] Greenhalgh D. A. and Jermy M., "Laser diagnostic for droplet measurements for the study of fuel injection and mixing in gas turbines and IC engine", *Applied Combustion Diagnostics*, pp. 408–428, 2002.

[14] Park S., Cho H., Yoon I. and Min K., Measurement of droplet size distribution of gasoline direct injection spray by droplet generator and planar image technique, *Measurement Science and Technology*, vol. 13, pp. 859–864, 2002.

[15] Greenhalgh D. A., " Laser imaging of fuel injection systems and combustors", *Proc. IMechE*, vol. 214, part A, pp-367-376, 2000

[16] Lockett R.D., Richter J. and Greenhalgh D. A., The Characterisation of a Diesel Spray Using Combined Laser Induced Fluorescence and Laser Sheet Dropsizing, *CWC2, Proceeding of the CLEO/Europe '98*, 1998.

[17] Kohse-Hoinghaus K. and Jeffries J. B., Applied Combustion Diagnostics, *Taylor & Francis*, 2002.

[18] Domann R. and Hardalupas Y., Quantitative Measurement of planar Droplet Sauter Mean Diameter in sprays using Planar Droplet Sizing, *Eleventh International Symposium on Application of Laser Techniques to Fluid Mechanics*, Lisbon, Portugal, July 2002.

[19] Kashdan J. T., Shrimpton J. S., Whybrew A., "Two-phase flow characterization by automated digital image analysis. part 1: Fundamental principles and calibration of the technique", *Part. Part. Syst. Charact.*, vol. 20, pp. 387–397, 2003.

[20] Kashdan J. T., Shrimpton J. S., Whybrew A., "Two-phase flow characterization by automated digital image analysis. Part 2: Application of PDIA for sizing sprays", *Part. Part. Syst. Charact.*, vol. 21, pp. 15–23, 2004.

[21] Kim J. H., Moon B. S., Rhim J. R., No S. Y., Kim J. Y. and Baik S. K., "Spray Cone Angles of port Fuel Injectors by Different Measuring Techniques", *Eighth International Conference on liquid Atomization and Spray Systems*,

July 2000.

[22] Kim W. T., Lee S. G., Rho B. J. and Kang S. J., "On the intermittent Spray Characteristics", KSME International Journal, Vol 12, No. 5, pp. 907-916, 1998

[23] Sujith R. I. et al., "Ximager", *http://www.ae.iitm.ac.in/ ~sujith/ximager/index_files/page0001.htm*.

[24] O'Rourke P. J. and Amsden A. A., "The TAB Model for numerical Calculation of Spray Droplet Break-up", *SAE Paper 872089*, 1987.

[25] O'Rourke P. J. And Bracco F. V., "Modelling of Drop Interactions in Thick Sprays and a Comparison with Experiment", *Strafied Charge Automitive Engines Conf.,* IMechE, London, 1980.

[26] Zimmer L., Fujimoto K., Ikeda Y. and Nakajima T., "Fuel droplet dynamics and cluster formation in an industrial oil burner by Planar Droplet Sizing", *11th International Symposium on Applications of Laser Techniques to Fluid Mechanics*, July 2002.

[27] Jermy M. C. and Greenhalgh D. A., "Planar Dropsizing by Elastic and Fluorescence Scattering in Sprays too Dense for Phase Doppler Measurement", *Appl. Phys. B*, vol. 71, pp. 703–710, 2000.